

## SUPPORTING INFORMATION

### **Background-free fluorescence decay time sensing and imaging of pH with highly photostable diazaoxotriangulenium dyes**

**Irene Dalfen,<sup>1</sup> Ruslan I. Dmitriev,<sup>2,3</sup> Gerhard Holst,<sup>4</sup> Ingo Klimant,<sup>1</sup> Sergey M. Borisov<sup>1\*</sup>**

1. Institute of Analytical Chemistry and Food Chemistry, Graz University of Technology,  
Stremayrgasse 9, 8010 Graz, Austria

2. School of Biochemistry and Cell Biology, University College Cork, Cork, Ireland

3. Institute for Regenerative Medicine, I.M. Sechenov First Moscow State University, Moscow,  
Russian Federation

4. PCO AG, Donaupark 11, 93309 Kelheim, Germany

\* sergey.borisov@tugraz.at

## **Table of Contents**

<b>Additional experimental data.....</b>	<b>3</b>
<b>Analytical data for structure analysis.....</b>	<b>4</b>
<b>Details on optode characterization.....</b>	<b>18</b>
<b>References .....</b>	<b>27</b>

## Additional experimental data

### Synthesis of tris(2,6-dimethoxyphenyl)methanol (a)

Phenyllithium was prepared from lithium (0.775 g, 111 mmol) and bromobenzene (4.8 mL, 46 mmol) in 40 mL Et<sub>2</sub>O and 4.6 mL (35 mmol) of 1,3-dimethoxybenzene were added. The reaction mixture was stirred overnight, after which 5.016 g (0.15 eq., 17 mmol) of 2,2',6,6'-tetramethoxybenzophenone dissolved in 50 mL hot toluene were added under Argon. The mixture was refluxed for two days and then poured into 150 mL H<sub>2</sub>O. The organic phase was extracted using DCM and the solvent was evaporated. Purification was achieved by precipitating from toluene by adding cyclohexane.

<sup>1</sup>H NMR (300 MHz, CDCl<sub>3</sub>): δ = 7.04 (t, J = 8.2 Hz, 3 H, arom. C-H), 6.49 (d, J = 8.2 Hz, 6 H, arom. C-H), 3.44 (s, 17 H, O-CH<sub>3</sub>).

<sup>13</sup>C APT-NMR (76 MHz, CDCl<sub>3</sub>): δ = 158.71, 127.43, 126.33, 106.99, 106.23, 77.16, 56.43.

### Preparation of nanoparticles

Nanoparticles were prepared via nanoprecipitation method. Polymer (RL-100 or PMMA-MA) and dye (0.75% wt. in respect to the polymer) were dissolved in acetone (0.2% wt. solution of the polymer) and the solution poured into a larger volume of water under vigorous stirring as described previously.<sup>1,2</sup> The aqueous dispersion of RL-100 nanoparticles was concentrated to final concentrations of 1.44 mg mL<sup>-1</sup> and 1.30 mg mL<sup>-1</sup> for PhOHCl<sub>2</sub>- and PhOHCl-DAOTA respectively. PMMA-MA nanoparticles were produced with PhOHCl-DAOTA only, with a final concentration of 1.0 mg mL<sup>-1</sup>.

Nanogel of PhOHCl<sub>2</sub>-DAOTA in poly(4-styrenesulfonic acid) was prepared by dissolving the polymer (142 mg) in MeOH:H<sub>2</sub>O (72 mL:20 mL). The dye (1.1 mg, 0.77% wt. in respect to the polymer) was dissolved in 15 mL of MeOH and added to the polymer solution under stirring. 400 mL of H<sub>2</sub>O were added quickly under vigorous stirring and the solvent evaporated until a concentration of approx. 1.32 mg mL<sup>-1</sup> was reached.

# Analytical data for structure analysis

Analytical data of tris(2,6-dimethoxyphenyl)methanol:

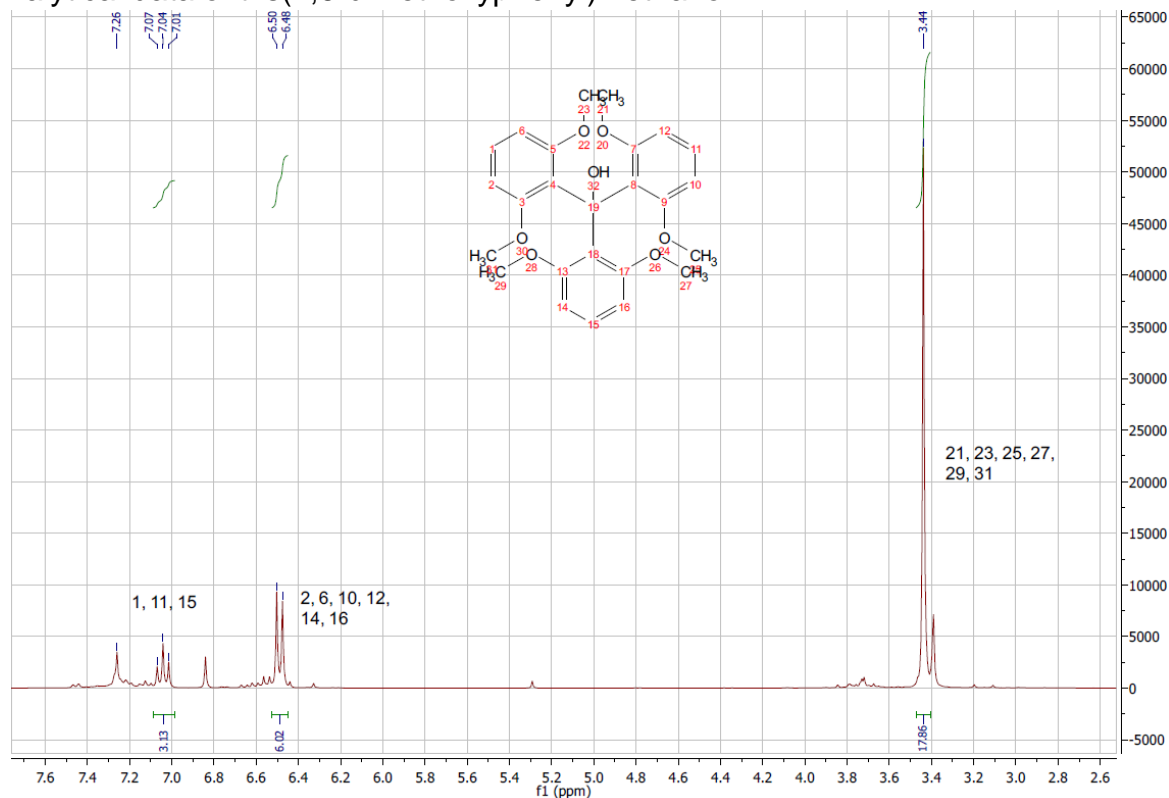


Figure S 1:  $^1\text{H}$  NMR spectrum ( $\text{CDCl}_3$ , 300 MHz) of tris(2,6-dimethoxyphenyl)methanol.

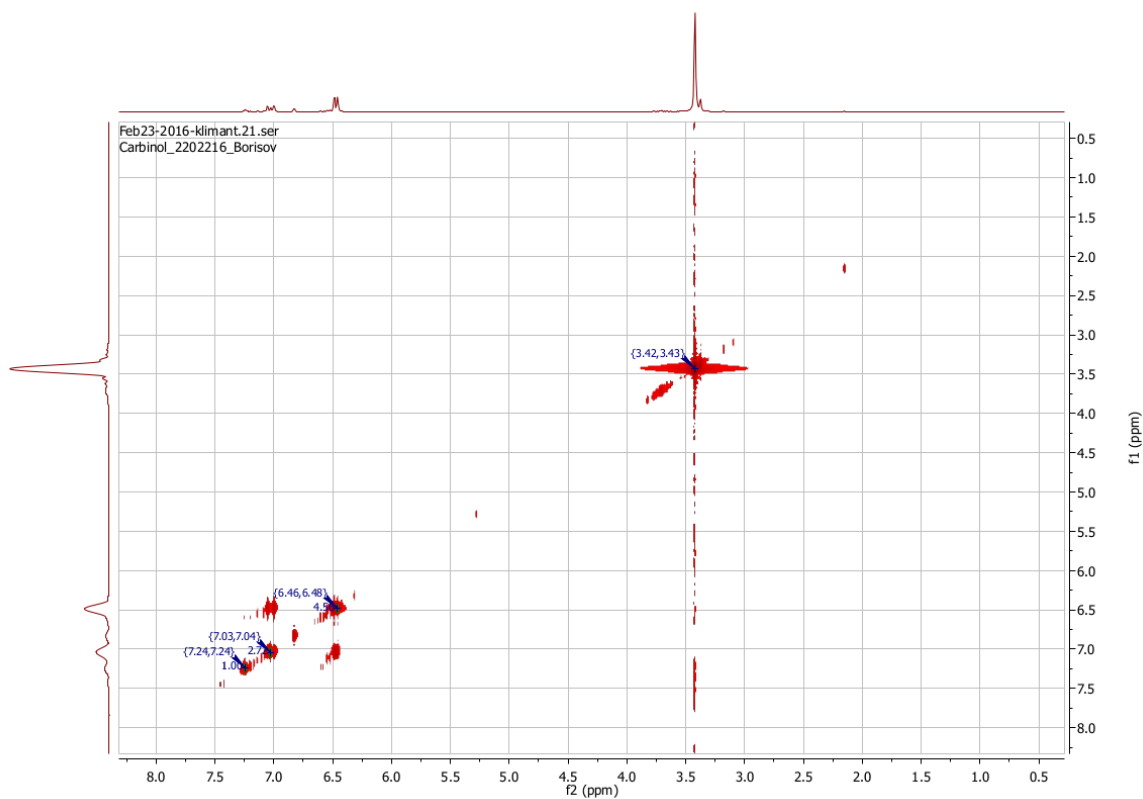
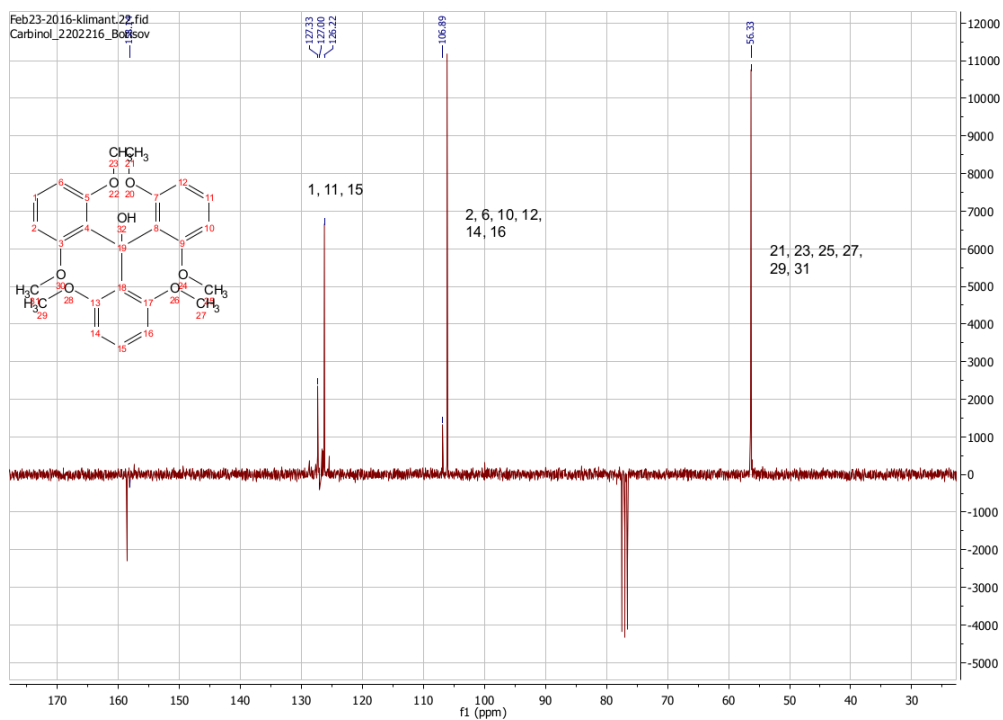
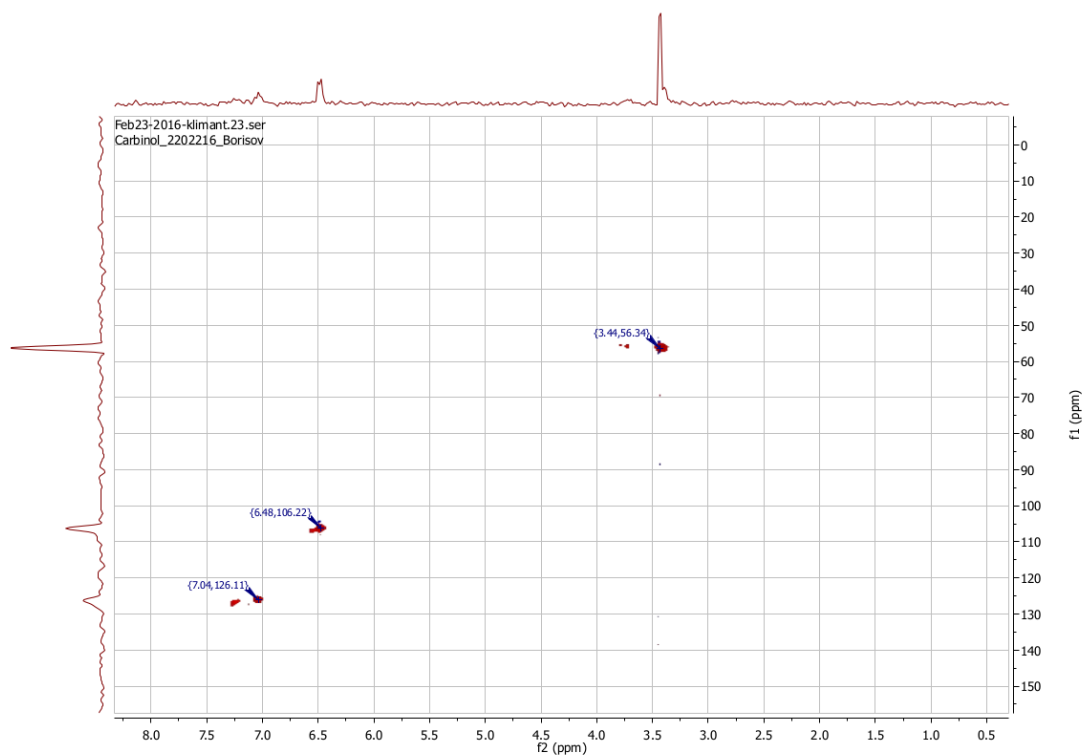


Figure S 2: COSY-NMR spectrum ( $\text{CDCl}_3$ , 300 MHz) of tris(2,6-dimethoxyphenyl)methanol.



**Figure S 3:**  $^{13}\text{C}$  APT-NMR spectrum ( $\text{CDCl}_3$ , 76 MHz) of tris(2,6-dimethoxyphenyl)methanol.



**Figure S 4:** HSQC-NMR spectrum of tris(2,6-dimethoxyphenyl)methanol in  $\text{CDCl}_3$ .

Analytical data of *N*-(3,5-dichloro-4-hydroxy)-*N*-dodecyl DAOTA<sup>+</sup> PF<sub>6</sub><sup>-</sup> (PhOHCl<sub>2</sub>-DAOTA):

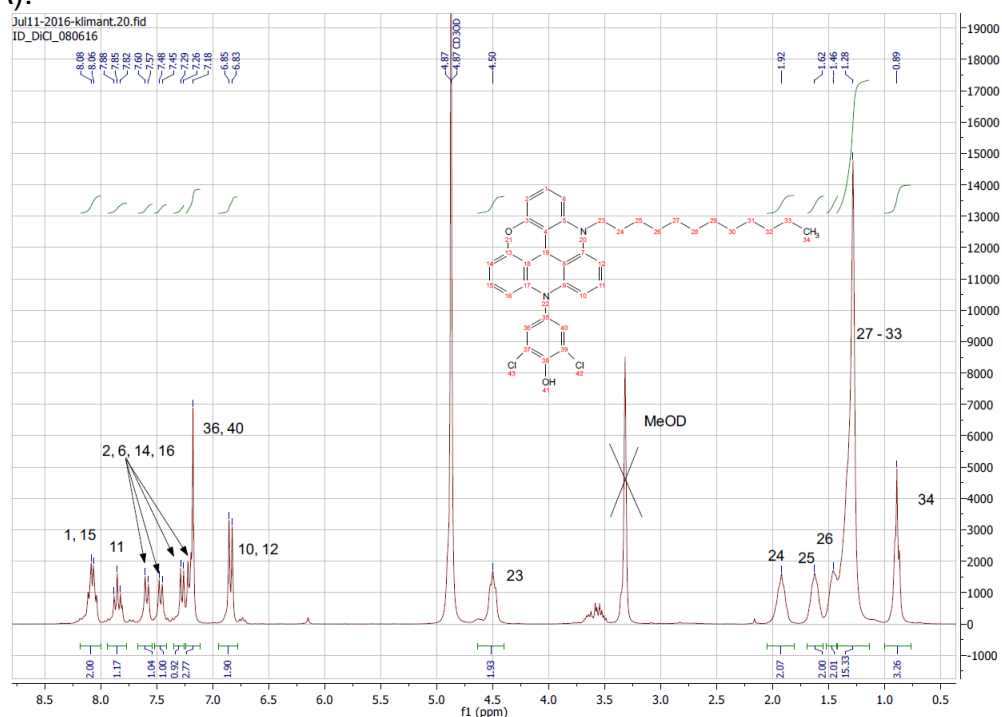


**Figure S 5:** <sup>1</sup>H NMR spectrum (CD<sub>3</sub>OD, 300 MHz) of *N*-(3,5-dichloro-4-hydroxy)-*N*-dodecyl DAOTA<sup>+</sup>.

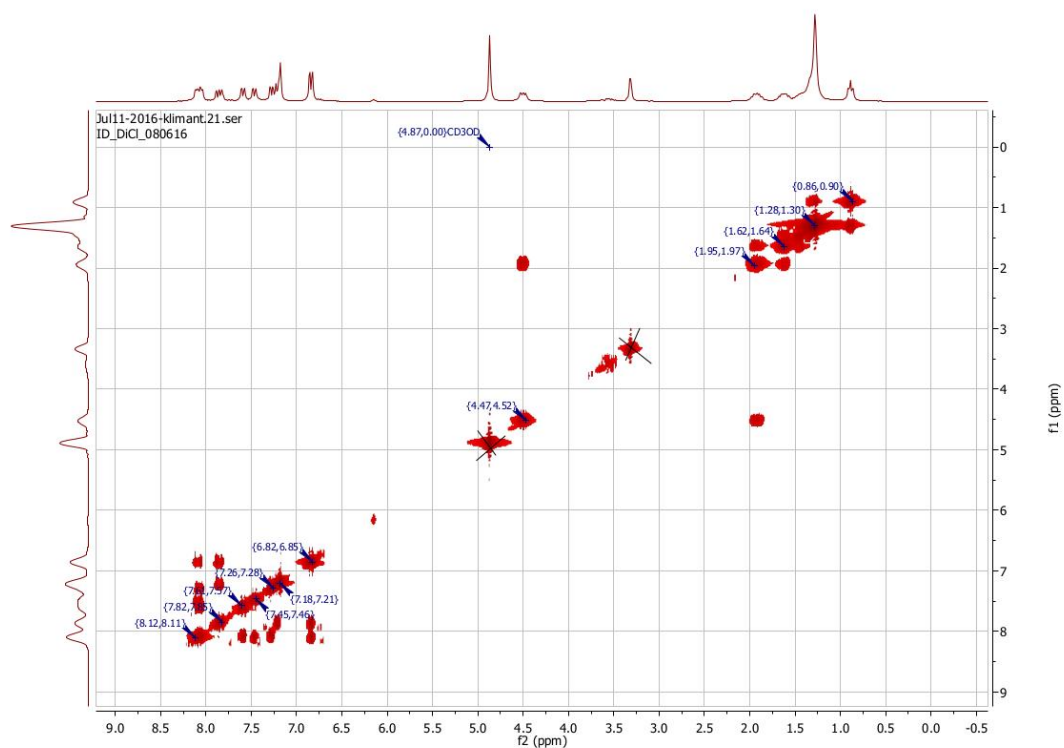


**Figure S 6:** COSY-NMR spectrum (CD<sub>3</sub>OD, 300 MHz) of *N*-(3,5-Dichloro-4-hydroxyphenyl)-*N*-dodecyl DAOTA<sup>+</sup>.

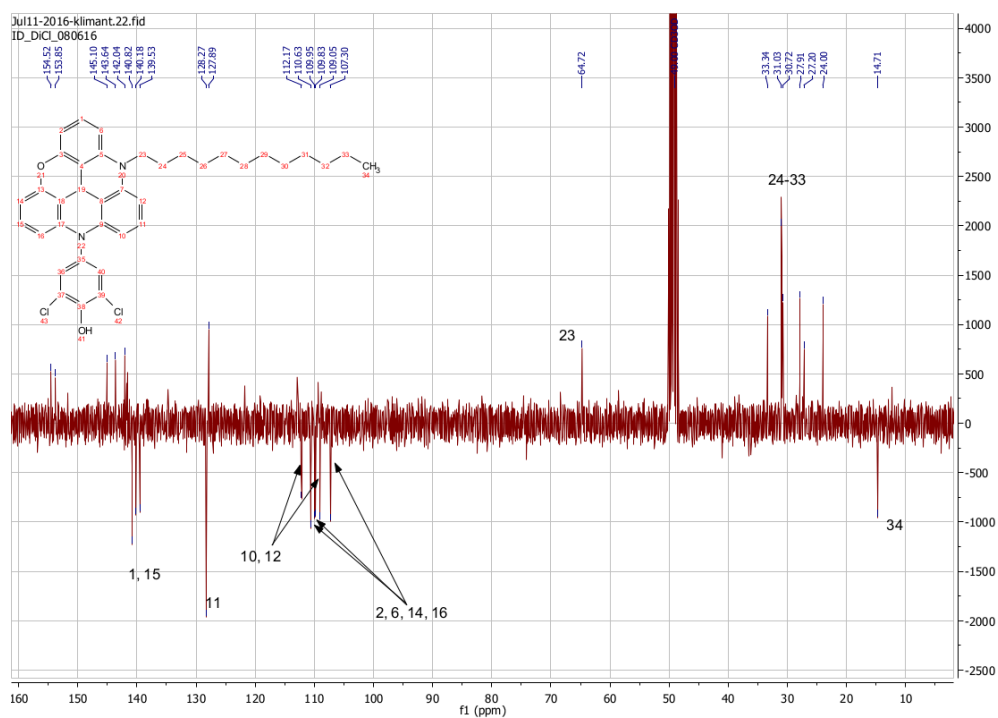


**Figure S 7:**  $^{13}\text{C}$  APT-NMR spectrum ( $\text{CD}_3\text{OD}$ , 76MHz) of *N*-(3,5-Dichloro-4-hydroxyphenyl)-*N*-dodecyl DAOTA $^+$ .

APT-NMR (76 MHz,  $\text{CD}_3\text{OD}$ ):  $\delta = 145.10, 143.64, 142.04, 140.82, 140.18, 139.53, 128.27, 127.89, 112.17, 110.63, 109.95, 109.05, 107.30, 64.72, 49.00, 33.34, 31.03, 30.72, 27.91, 27.20, 24.00, 14.71$

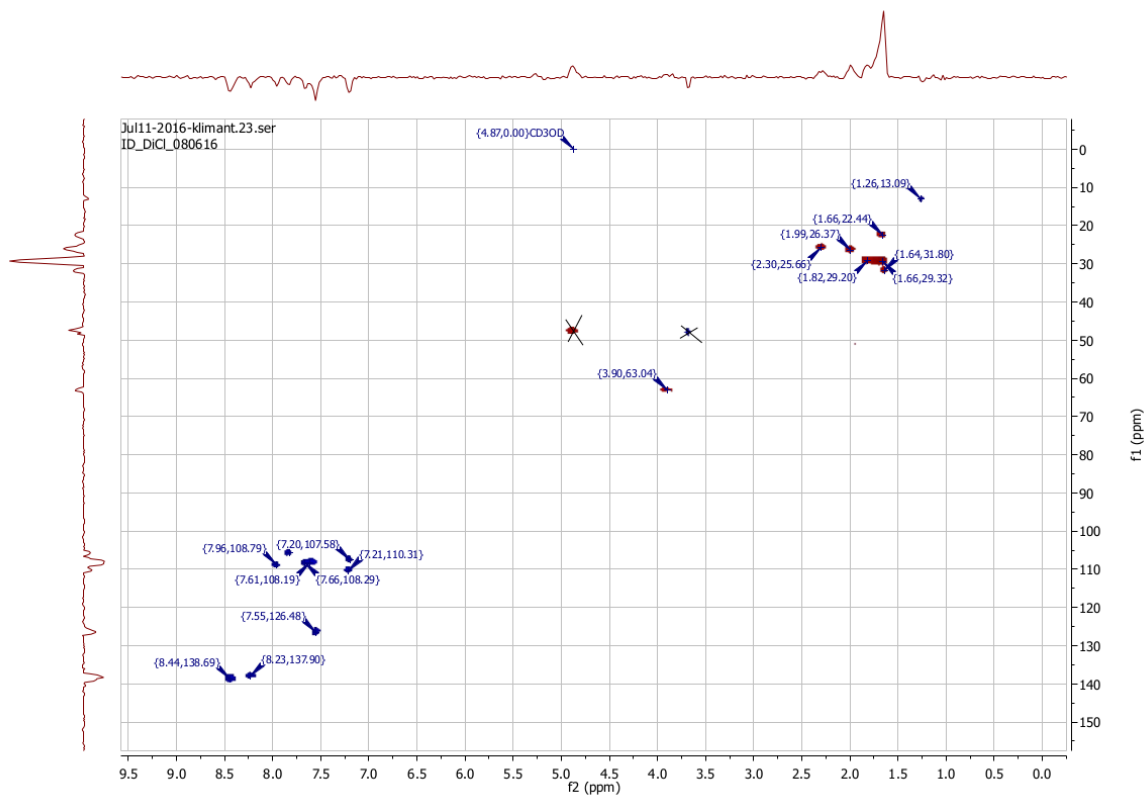


**Figure S 8:** HSQC-NMR spectrum of *N*-(3,5-Dichloro-4-hydroxyphenyl)-*N*-dodecyl DAOTA<sup>+</sup> in CD<sub>3</sub>OD.

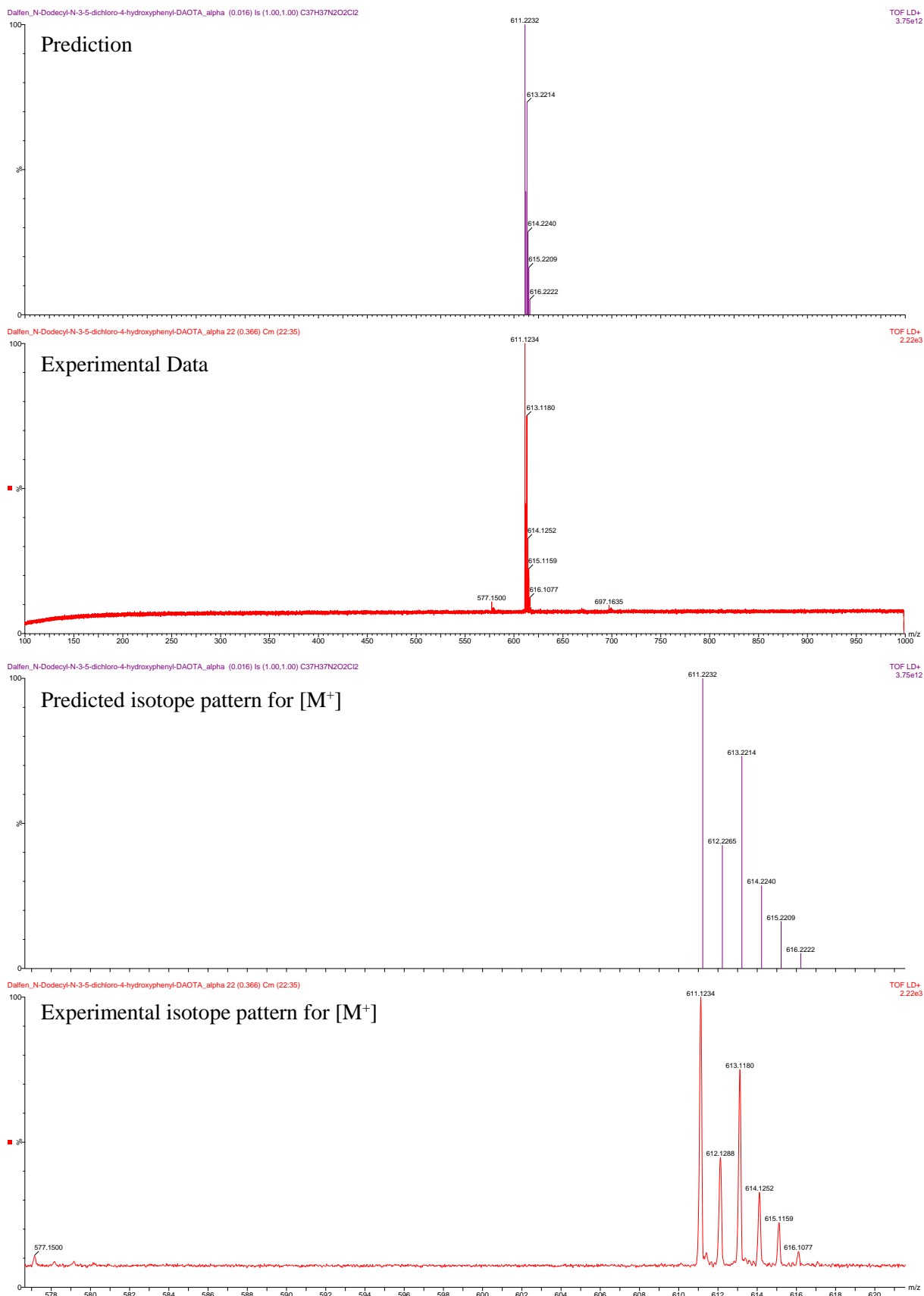


**Figure S 9:** MS MALDI-TOF spectrum of *N*-(3,5-Dichloro-4-hydroxyphenyl)-*N*-dodecyl DAOTA<sup>+</sup> (**Top**); calculated and experimental isotope patterns (**bottom**). *m/z* calculated: [M<sup>+</sup>] = 611.22, detected: [M<sup>+</sup>] = 611.12

Analytical data of *N*-(3-chloro-4-hydroxy)-*N*-dodecyl DAOTA<sup>+</sup> PF<sub>6</sub><sup>-</sup> (PhOHCl-DAOTA):

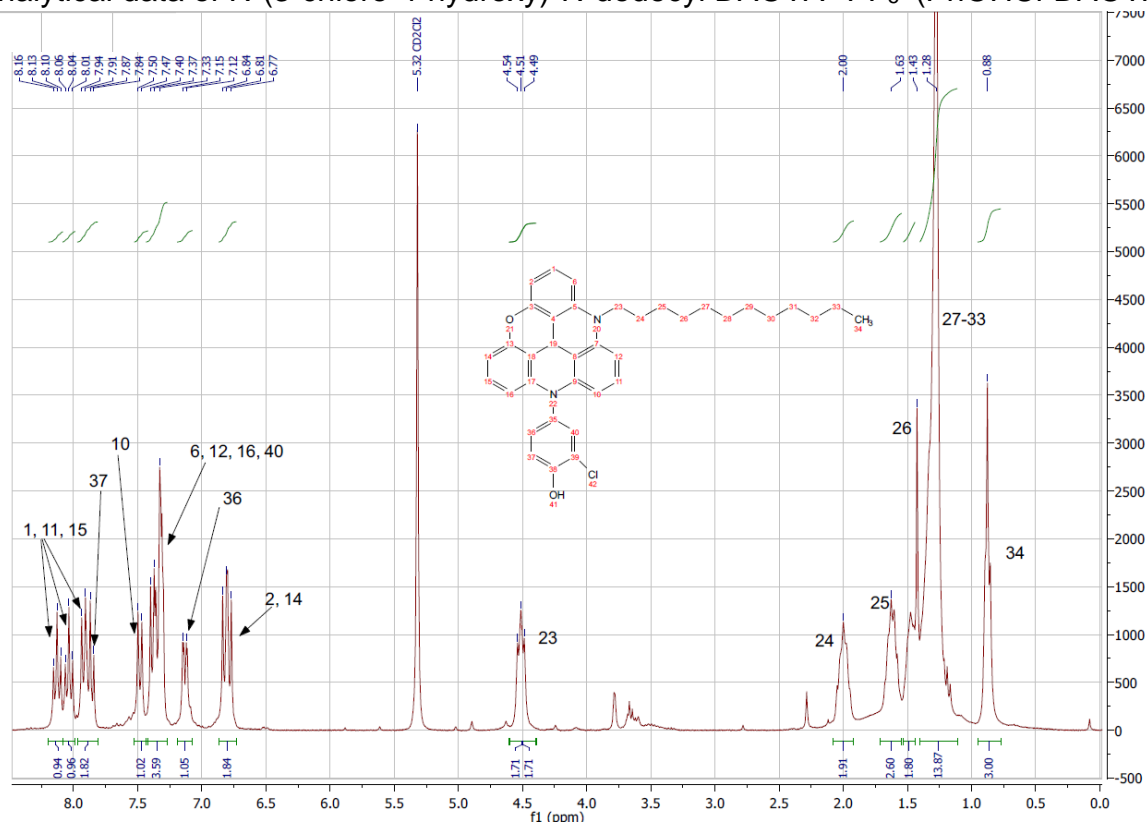


Figure S 10: <sup>1</sup>H NMR spectrum (CD<sub>2</sub>Cl<sub>2</sub>, 300 MHz) of *N*-(3-chloro-4-hydroxy)-*N*-dodecyl DAOTA<sup>+</sup>.

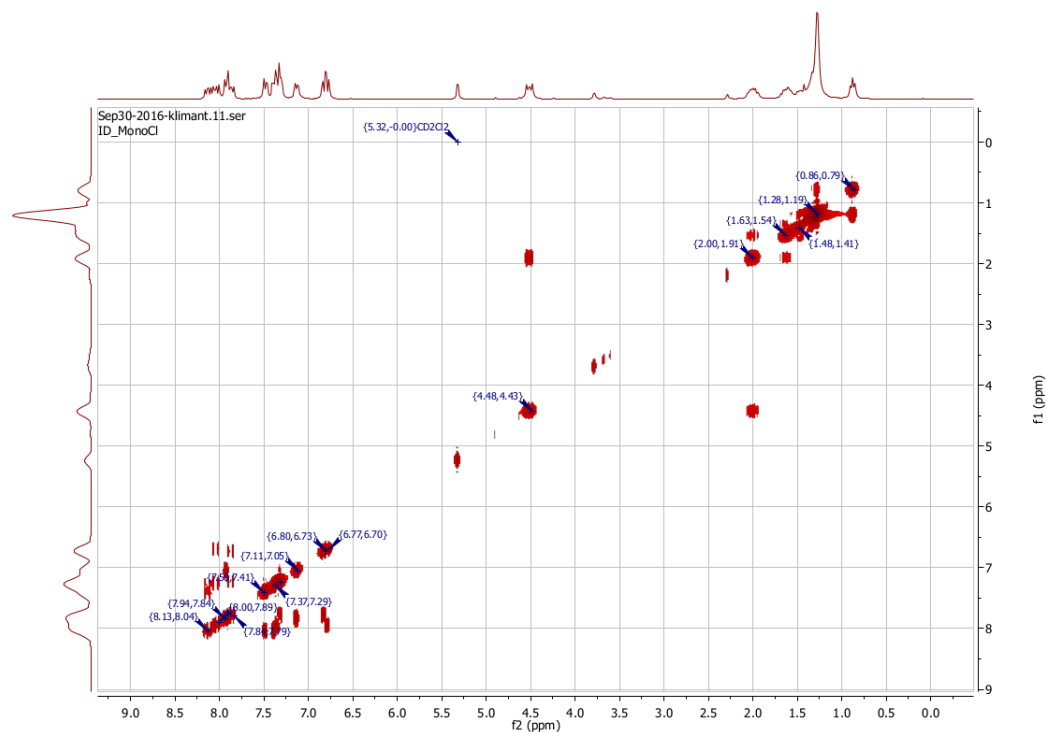
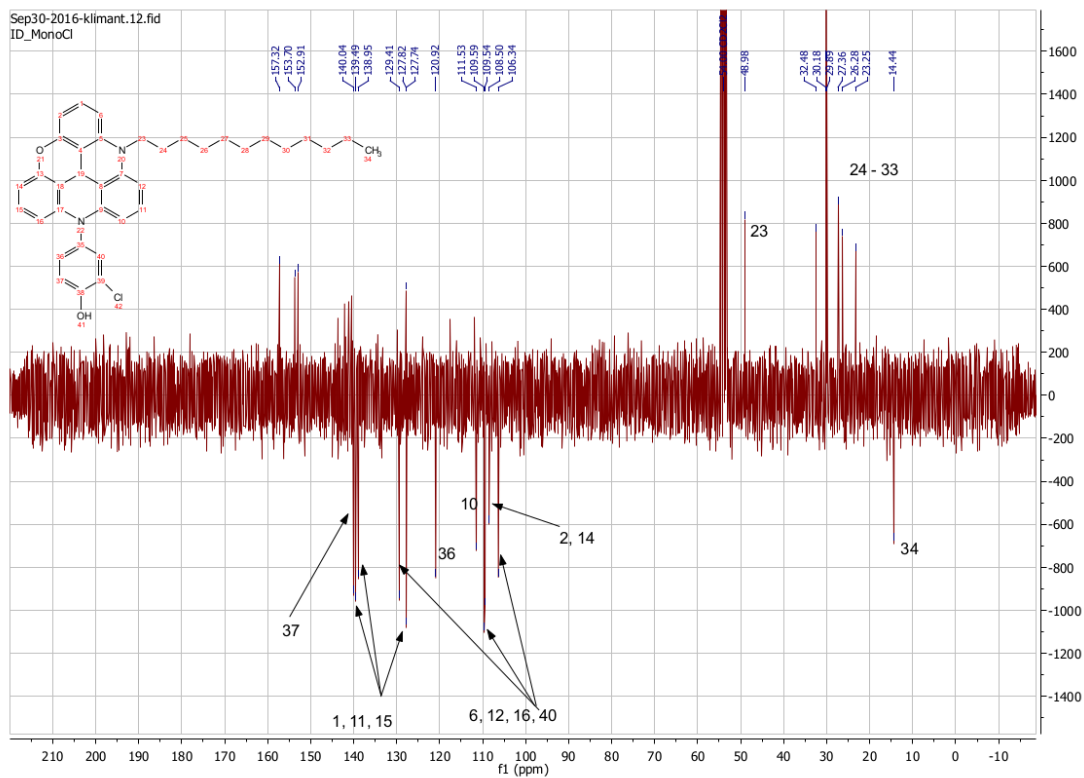
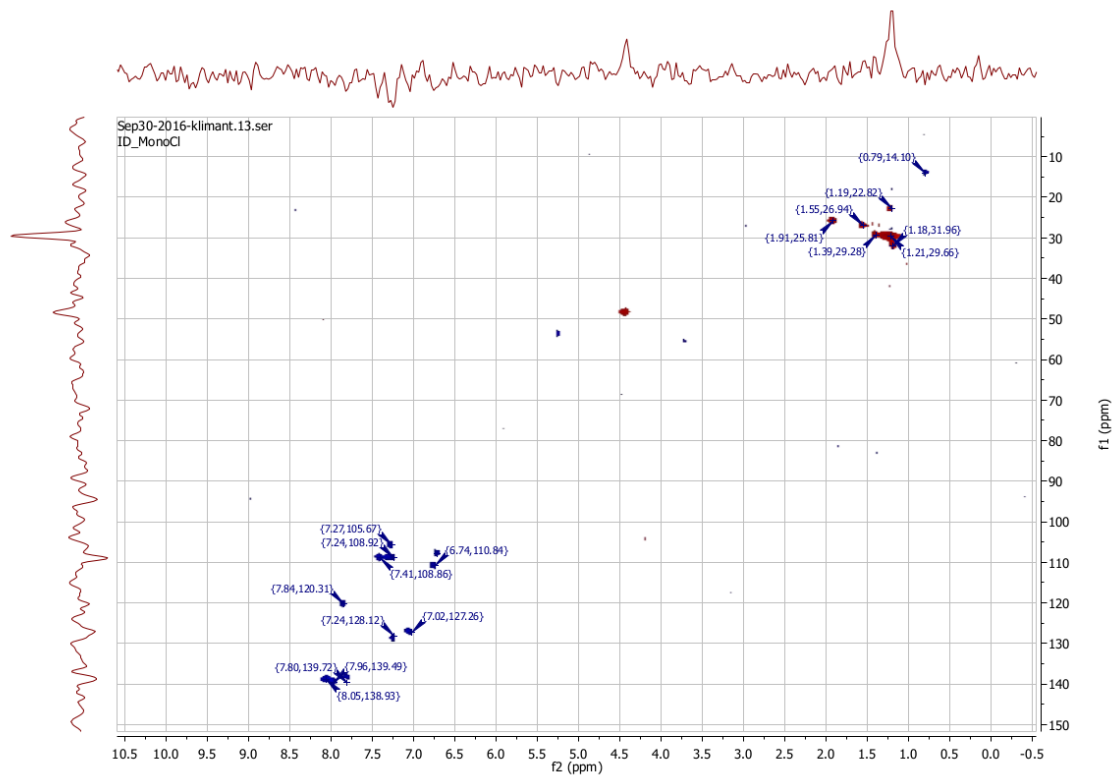


Figure S 11: COSY-NMR spectrum (CD<sub>2</sub>Cl<sub>2</sub>, 300 MHz) of *N*-(3-chloro-4-hydroxyphenyl)-*N*-dodecyl DAOTA<sup>+</sup>.



**Figure S 12:**  $^{13}\text{C}$  APT-NMR spectrum ( $\text{CD}_2\text{Cl}_2$ , 76 MHz) of *N*-(3-chloro-4-hydroxyphenyl)-*N*-dodecyl DAOTA<sup>+</sup>.

APT-NMR (76 MHz,  $\text{CD}_2\text{Cl}_2$ ):  $\delta = 145.10, 143.64, 142.04, 140.82, 140.18, 139.53, 128.27, 127.89, 112.17, 110.63, 109.95, 109.05, 107.30, 64.72, 49.00, 33.34, 31.03, 30.72, 27.91, 27.20, 24.00, 14.71$



**Figure S 13:** HSQC-NMR spectrum of *N*-(3-Chloro-4-hydroxyphenyl)-*N*-dodecyl DAOTA<sup>+</sup> in CD<sub>2</sub>Cl<sub>2</sub>.

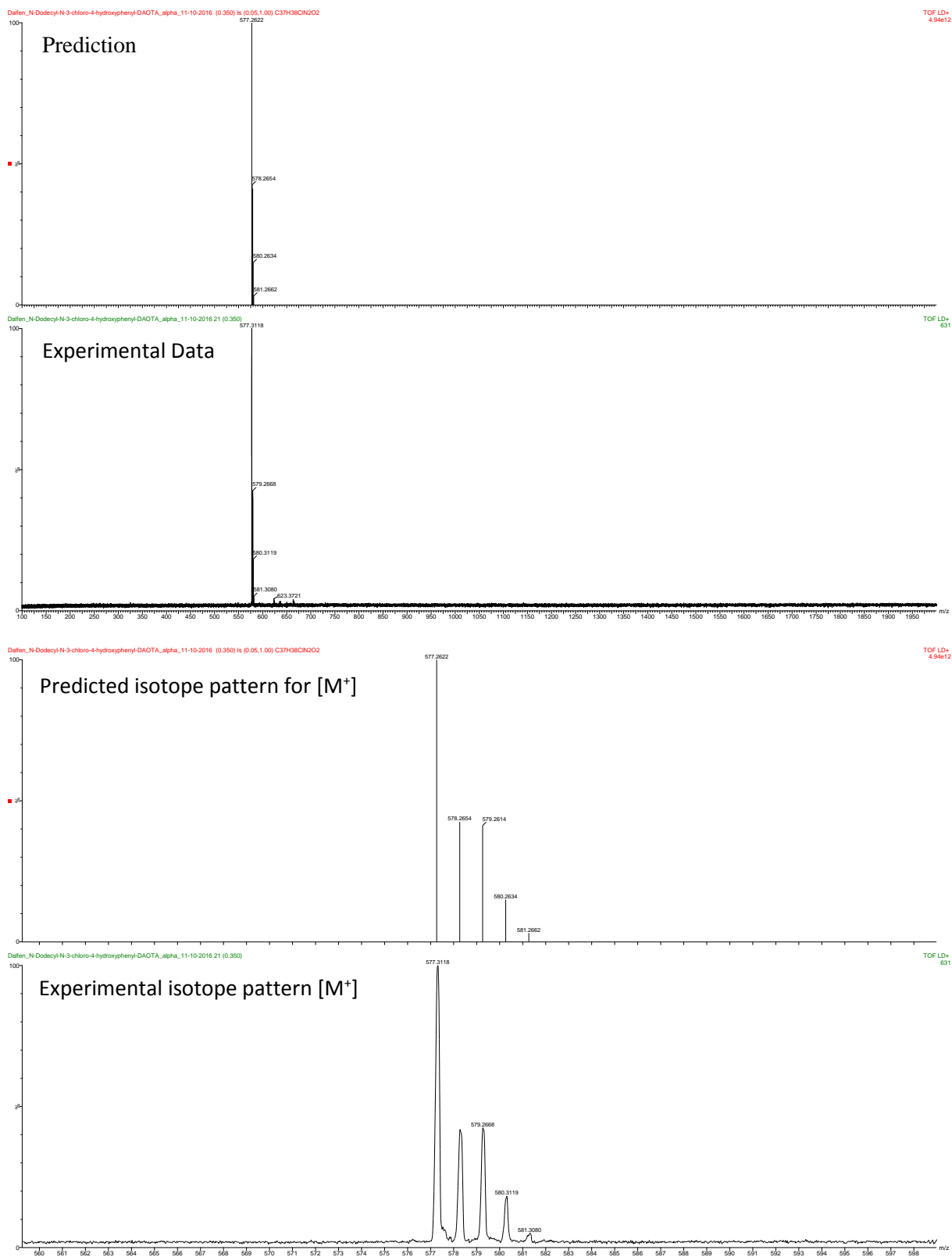


**Figure S 14:** MS MALDI-TOF spectrum of PhOHCl-DAOTA (**Top**); calculated and experimental isotope patterns (**bottom**).  $m/z$  calculated:  $[M^+] = 577.26$ , detected:  $[M^+] = 577.25$

Analytical data of *N*-(3-Morpholinopropyl)-*N*-dodecyl DAOTA<sup>+</sup> PF<sub>6</sub><sup>-</sup> (Morph-DAOTA):

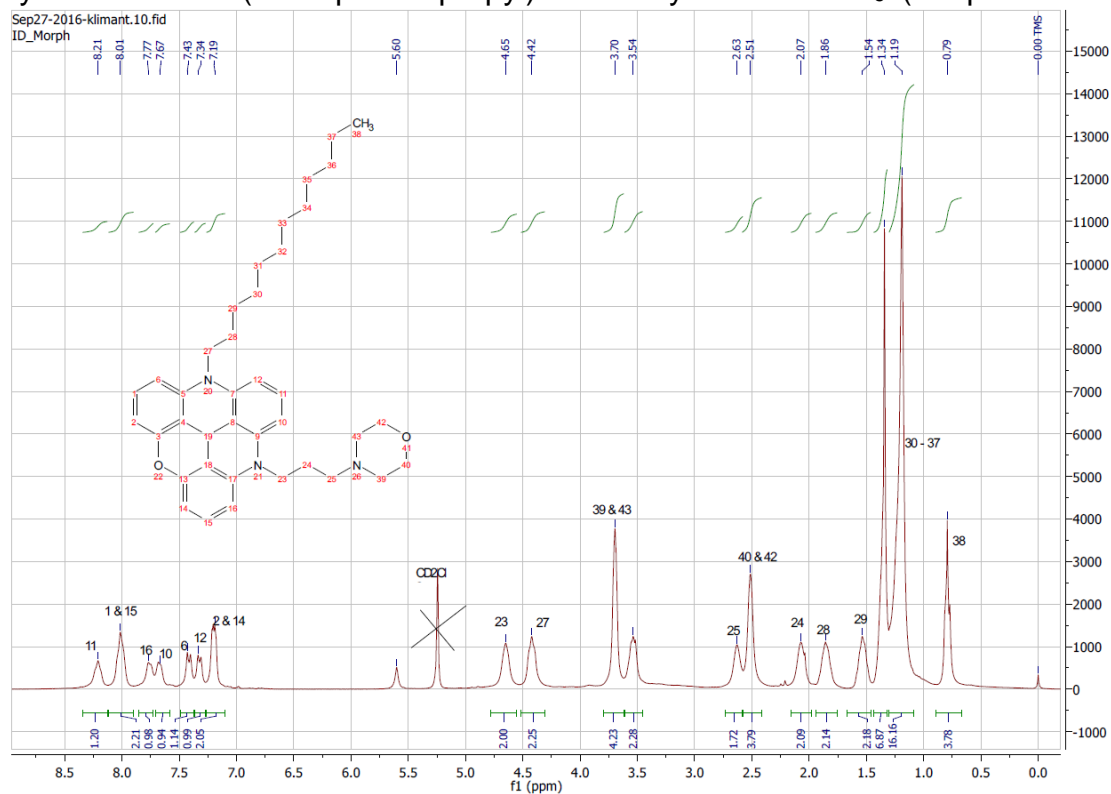


Figure S 15: <sup>1</sup>H NMR (CD<sub>2</sub>Cl<sub>2</sub>, 300 MHz) of *N*-(3-morpholinopropyl)-*N*-dodecyl DAOTA<sup>+</sup>.

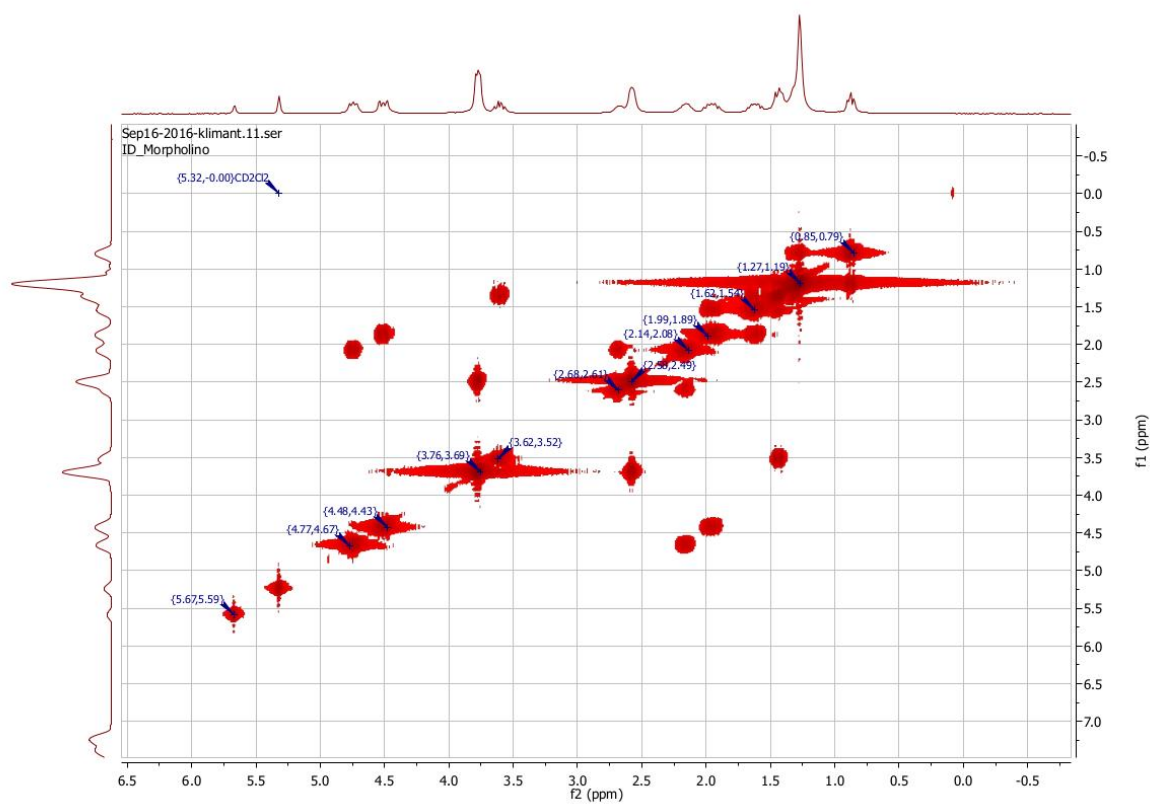
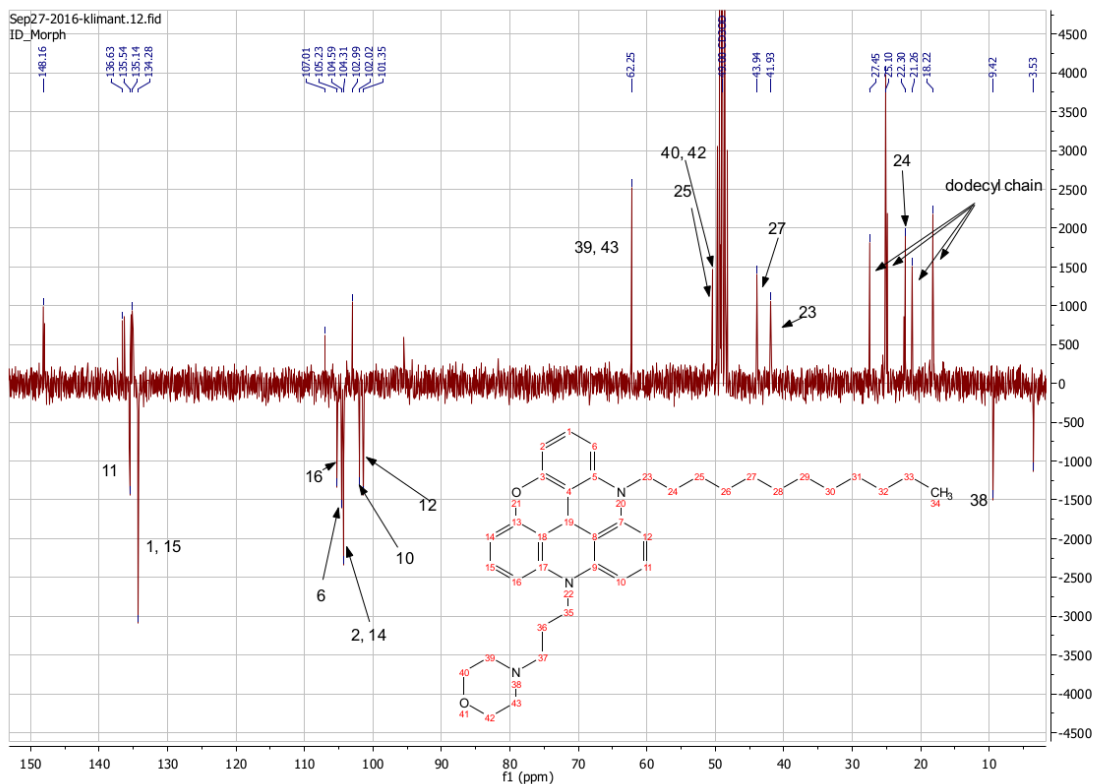
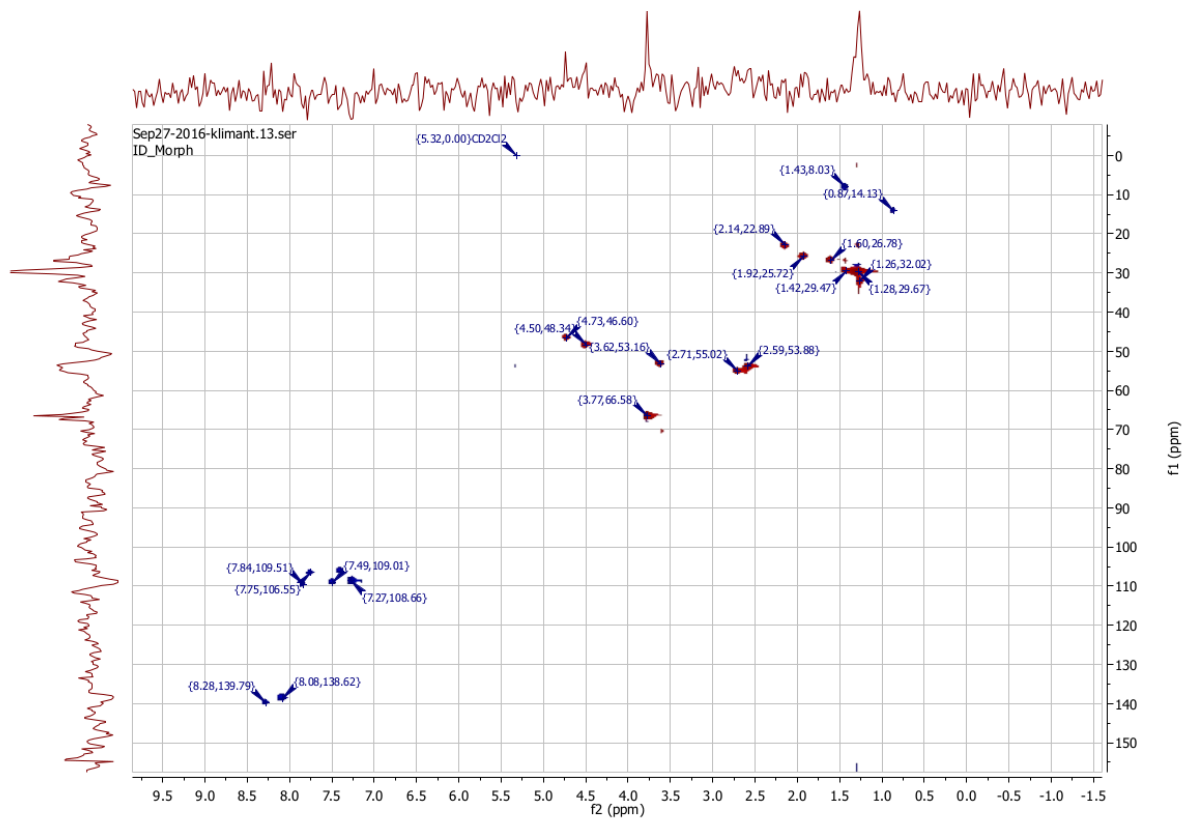


Figure S 16: COSY-NMR spectrum (CD<sub>2</sub>Cl<sub>2</sub>, 300 MHz) of *N*-(3-morpholinopropyl)-*N*-dodecyl DAOTA<sup>+</sup>.



**Figure S 17:** <sup>13</sup>C APT-NMR spectrum (CD<sub>2</sub>Cl<sub>2</sub>, 76MHz) of N-(3-morpholinopropyl)-N-dodecyl DAOTA<sup>+</sup>.

APT-NMR (76 MHz, CD<sub>2</sub>Cl<sub>2</sub>):  $\delta$  = 153.16, 141.63, 141.30, 140.54, 140.39, 140.14, 139.28, 112.01, 110.23, 109.59, 109.29, 107.99, 107.02, 106.35, 100.54, 67.25, 54.00, 48.94, 46.93, 32.45, 30.10, 29.87, 27.30, 26.26, 23.22, 14.42, 8.53



**Figure S 18:** HSQC-NMR spectrum of *N*-(3-morpholinopropyl)-*N*-dodecyl DAOTA<sup>+</sup> in CD<sub>2</sub>Cl<sub>2</sub>.

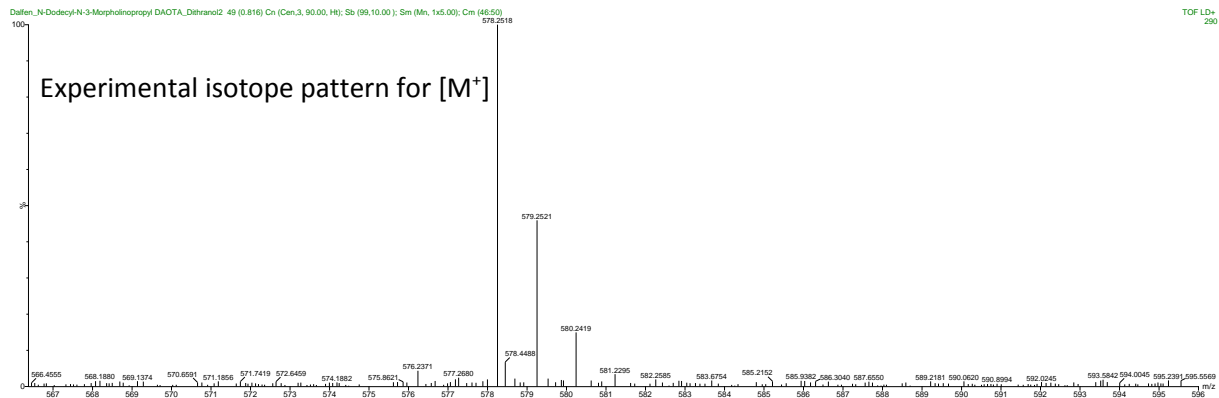
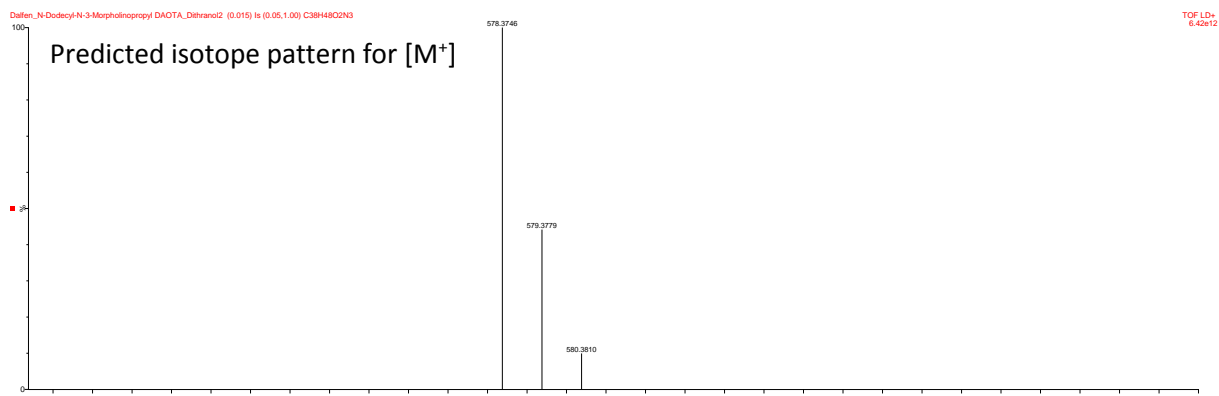
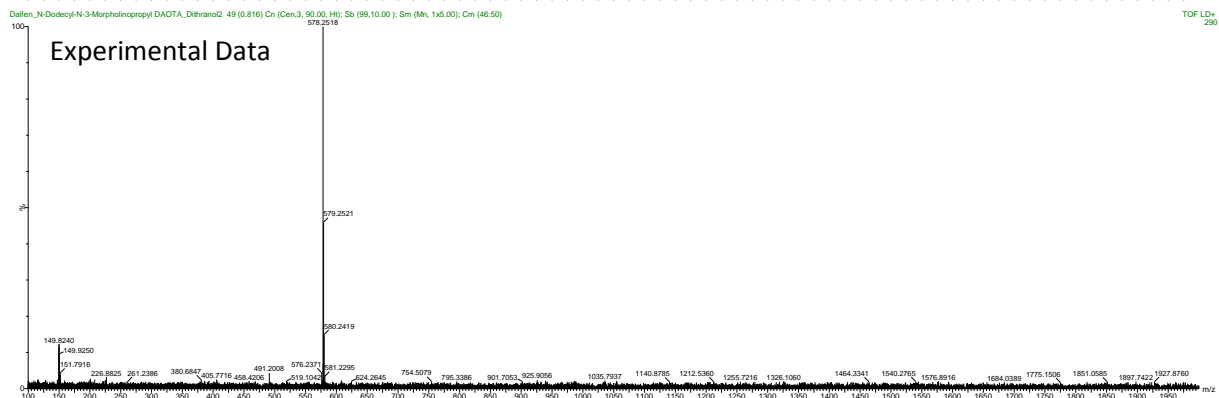
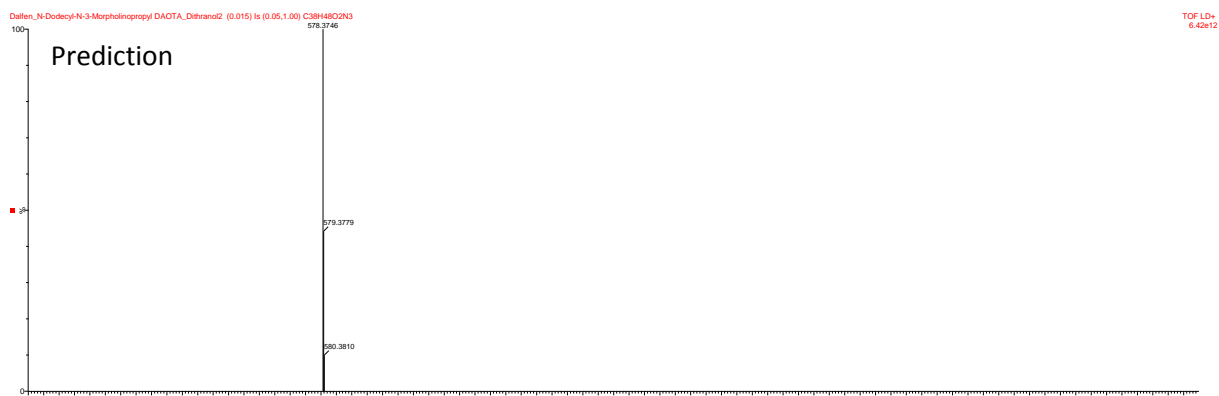


**Figure S 19:** MS MALDI-TOF spectrum of *N*-(3-morpholinopropyl)-*N*-dodecyl DAOTA<sup>+</sup> (**Top**); calculated and experimental isotope patterns (**bottom**). *m/z*. calculated: [M<sup>+</sup>] = 578.37, detected: [M<sup>+</sup>] = 578.25

## Details on optode characterization

Effect of chloride ions on fluorescence in solution

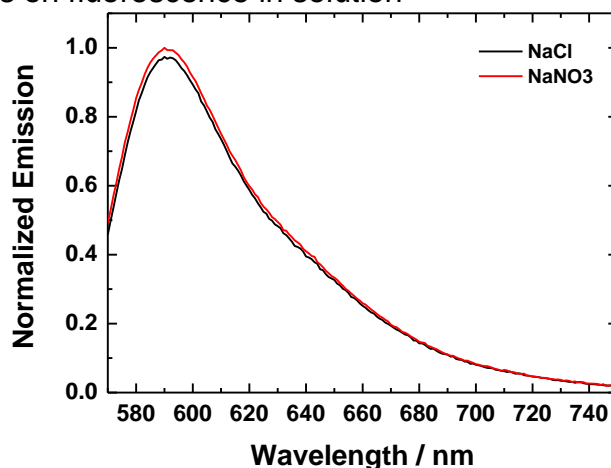


**Figure S 20:** Emission spectra of PhOHCl<sub>2</sub>-DAOTA at pH 3 in EtOH:buffer solutions with 10 mM buffer concentration (Acetate:phosphate:TRIS 1:1:1) and 290 mM NaCl or NaNO<sub>3</sub>, respectively.

## Photostability

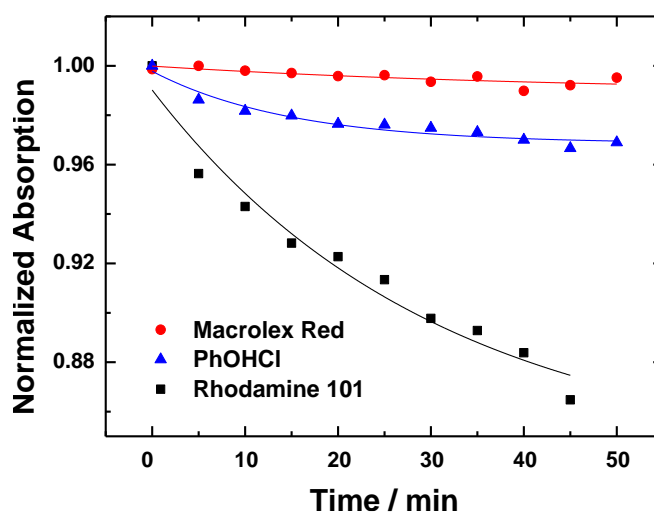


**Figure S 21:** Photodegradation of PhOHCl-DAOTA, Macrolex Red and Rhodamine 101 in EtOH solutions upon illumination with high power LED array ( $\lambda = 528$  nm, Absorption measured at 560 nm).

## Hysteresis/Reversibility

The response time, reversibility and hysteresis were determined via fluorescence intensity measurement with lock-in amplifier in buffers with an ionic strength of 150 mM (10 mM buffer concentration, 140 mM NaCl). The sensor foil attached to the distal end of the fiber was switched between the buffers with pH above and below the apparent  $pK_a$  value of the dye (pH 4 and 6 for PhOHCl<sub>2</sub>-DAOTA; pH 6 and 8 for PhOHCl-DAOTA).

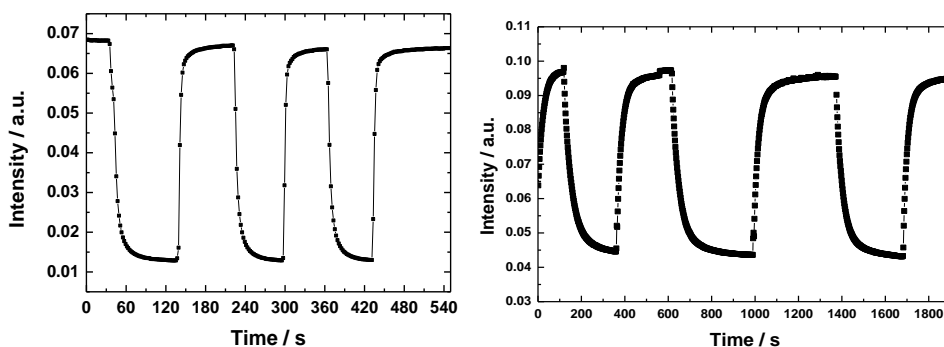


**Figure S 22:** *Left and right:* response of PhOHCl<sub>2</sub>-DAOTA and PhOHCl-DAOTA, respectively, immobilized into D4 hydrogel (1% wt. of the dye) to variation of the pH of the buffer solution.

#### pH dependence of Morph-DAOTA in D4

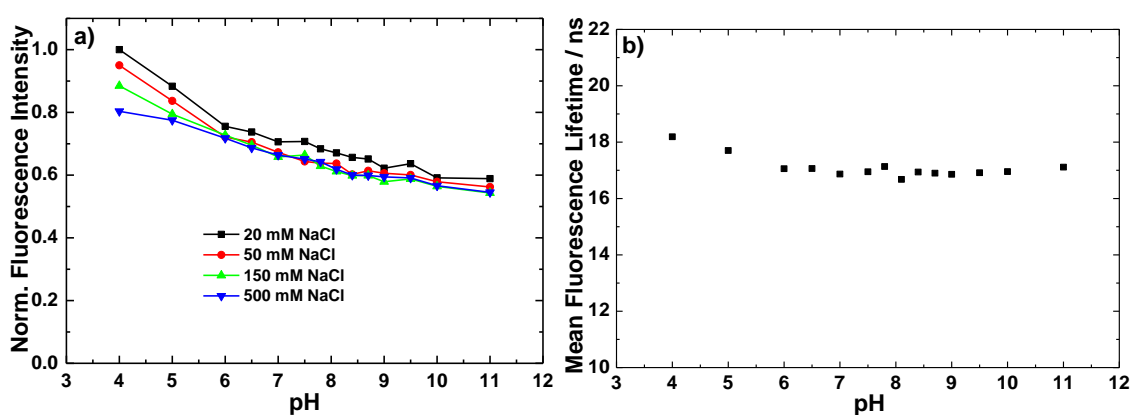


**Figure S 23:** pH dependence of the fluorescence intensity (a) and fluorescence decay time (b) for the sensing foil based on Morph-DAOTA in D4 (1% wt.). Buffer concentration was always 10 mM, for (a) the ionic strength was set to the values indicated with NaCl, for (b) the ionic strength was set to 150 mM with NaCl.

#### Leaching experiments

To determine the stability of the dyes in various matrices, a sensor foil (1% wt. of PhOHCl<sub>2</sub>-DAOTA in D4) was positioned into a flow-through cell which was pumped through with buffers (pH 4 acetate buffer and pH 6.5 phosphate buffer, buffer concentration of 10 mM and ionic strength of 150 mM adjusted with NaCl). The absorption of the sensor foil was measured continuously at the absorption maximum (560 nm).

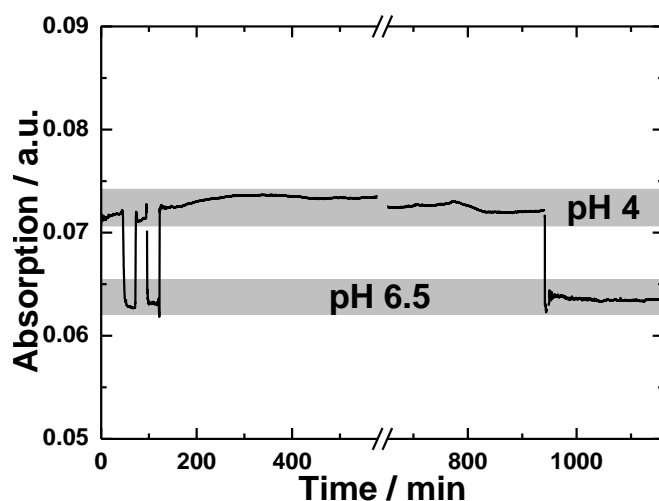


**Figure S 24:** Leaching experiment for  $\text{PhOHCl}_2\text{-DAOTA}$  embedded into hydrogel D4 (1% wt. of the dye).

### Effect of metal cations and hydrogen peroxide

The potential cross sensitivity to common metal cations was investigated for  $\text{PhOHCl}_2\text{-DAOTA}$  sensor foils with 1% wt. dye in D4 in buffers at pH 3 with 10 mM buffer concentration and 140 mM NaCl as background electrolyte. The emission intensity and lifetime of the foils in this buffer (reference) were compared to the parameters obtained in the buffer solutions spiked with 10 mM KCl, 10 mM  $\text{CaCl}_2$ , 100  $\mu\text{M}$   $\text{ZnCl}_2$  and 100  $\mu\text{M}$   $\text{CuCl}_2$  to investigate potential cross-sensitivity at physiologically relevant concentrations.

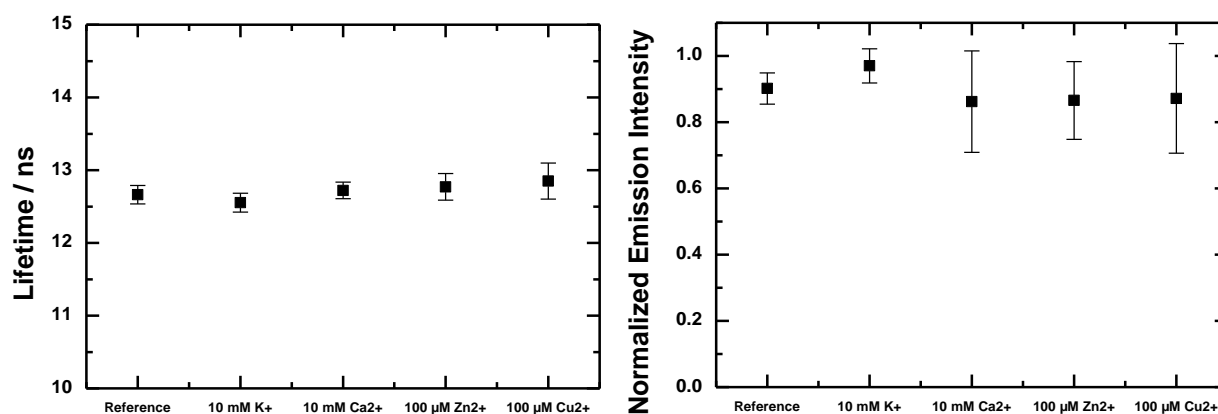


**Figure S 25:** Determination of selectivity of pH over common metal cations of  $\text{PhOHCl}_2\text{-DAOTA}$  1% wt. in D4; Buffer concentration 10 mM, background electrolyte: 140 mM NaCl. Metal cation concentrations as indicated in the graphs.

Likewise, cross-sensitivity to hydrogen peroxide as a representative of reactive oxygen species was tested by recording emission spectra of a planar optode of  $\text{PhOHCl}_2\text{-DAOTA}$  with and without hydrogen peroxide. The buffer solution with the foil was spiked with concentrated  $\text{H}_2\text{O}_2$  solution to result in the 1% vol. of  $\text{H}_2\text{O}_2$  in the investigated solution. The emission recorded during the following 10 minutes,

then the concentration of  $\text{H}_2\text{O}_2$  was increased to 2% vol. and again emission was measured over 10 minutes.

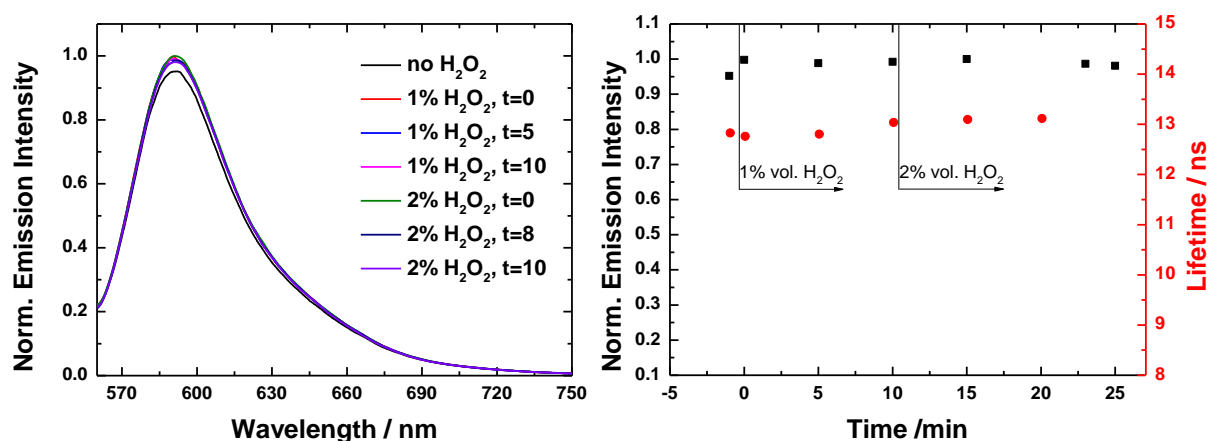


**Figure S 26:** Determination of cross-sensitivity to hydrogen peroxide. Buffer concentration 10 mM, background electrolyte: 140 mM NaCl, pH 3.

### Nafion/D4 hybrid optodes

In order to further investigate the behaviour of the indicators in the presence of anions of varying hydrophobicity, planar optodes of 1% wt.  $\text{PhOHCl}_2$  DAOTA in a matrix of 20% Nafion<sup>®</sup> 117 and 80% D4 were prepared. Calibrations of fluorescence intensity and decay times were performed in buffers with 10 mM buffer concentration and the ionic strength set to 20, 150 and 300 mM with NaCl as well as in buffers containing 100 mM  $\text{NaClO}_4$  and an overall ionic strength of 300 mM set with NaCl. The results show that in contrast to pure Hydrogel, hydrophobicity of anions in the solution has almost no influence on the calibration for the Nafion/D4 blends. It can be hypothesized that the dye forms stable ion pairs with the negatively charged sulfonic acid groups in the Nafion<sup>®</sup> polymer and therefore would not relocate to other domains anymore. On the other hand, due to highly charged character of Nafion, a stronger cross-sensitivity to ionic strength is observed.

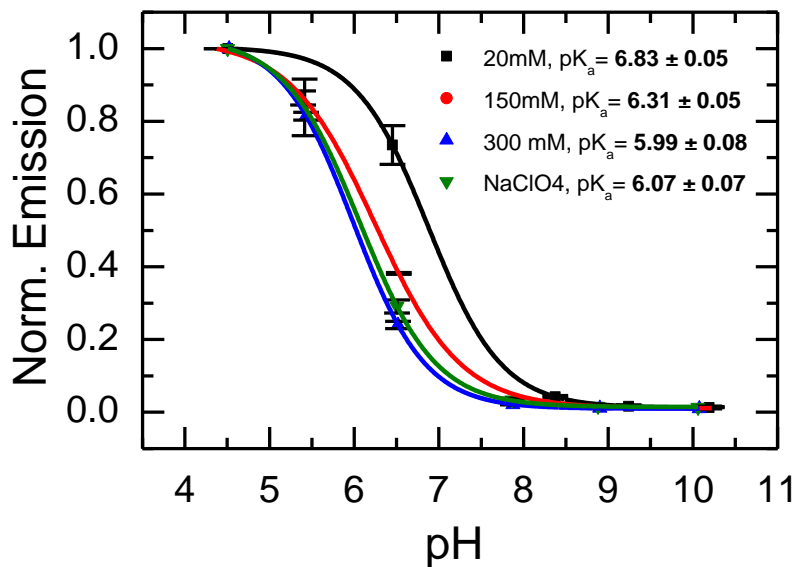


**Figure S 27:** Calibrations for the sensor based on  $\text{PhOHCl}_2$  DAOTA in Nafion:D4 blend (20:80 w/w) in buffers with 10 mM buffer concentration and the ionic strength set to 20, 150 and 300 mM set with NaCl as well as in buffers containing 100 mM  $\text{NaClO}_4$  and an overall ionic strength of 300 mM set with NaCl.

Data on decay time calibrations

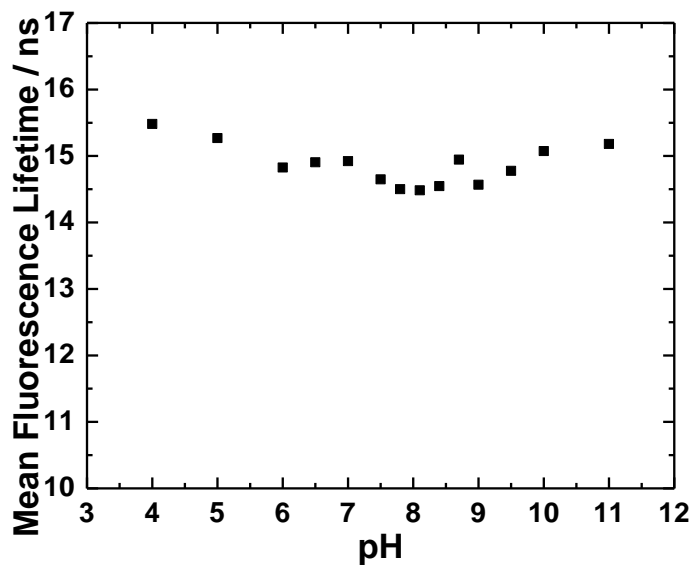


**Figure S 28:** Fluorescence decay time dependence on pH of  $\text{PhOHCl}$ -DAOTA in EtOH/buffer solution 1:1 (v/v). Dye concentration is 10  $\mu\text{M}$ , buffer concentration 10 mM and the ionic strength 150 mM set with NaCl.

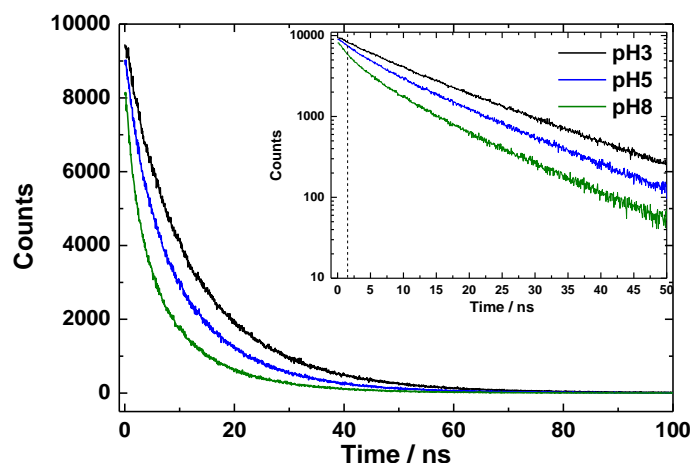


**Figure S 29:** Fluorescence decays of  $\text{PhOHCl}_2\text{-DAOTA}$  1% wt. in D4 in buffers with 10 mM buffer concentration and 140 mM NaCl; Inset: logarithmic plot with dotted line marking the cutoff point at 1.5 ns after the peak maximum.

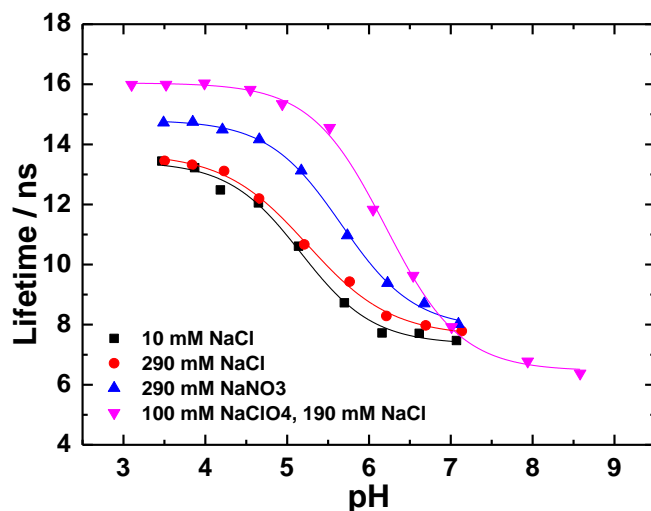


**Figure S 30:** pH response of the decay time of  $\text{PhOHCl}_2\text{-DAOTA}$  in D4 (1% wt.) in buffers with different concentration and nature of background electrolyte, buffer concentration always 10 mM. Inflection points:  $5.10 \pm 0.11$  (10 mM NaCl),  $5.23 \pm 0.08$  (290 mM NaCl),  $5.64 \pm 0.07$  (290 mM  $\text{NaNO}_3$ ) and  $6.20 \pm 0.01$  (100 mM  $\text{NaClO}_4$  plus 190 mM NaCl)

## Sensing properties of the indicators in nanoparticles

To investigate the pH response of the nanoparticles, the stock solution of the nanobeads was diluted 2-fold with the solution containing 20 mM of buffer and total ionic strength of 300 mM adjusted with NaCl.

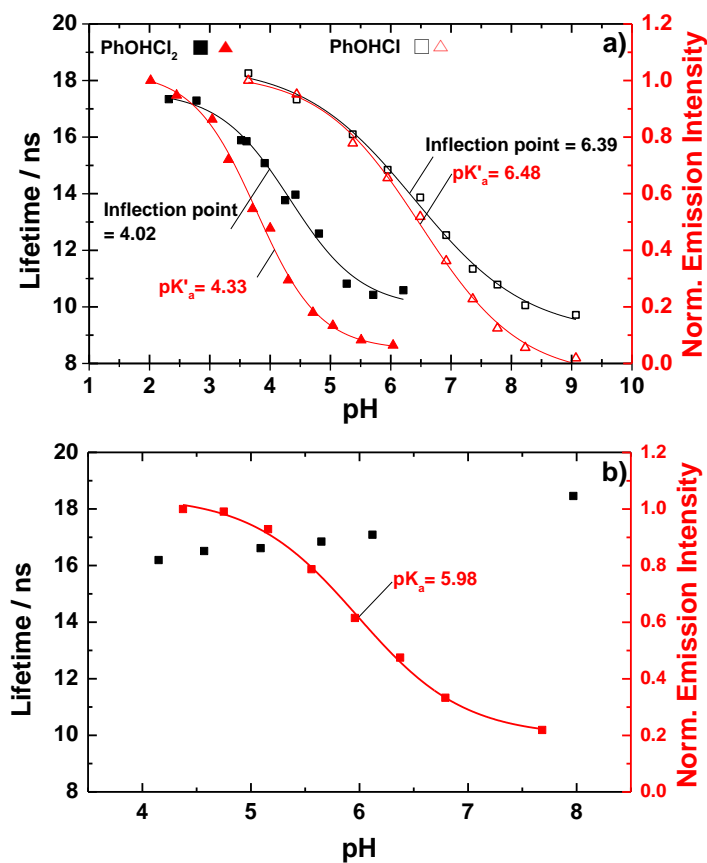


**Figure S 31:** a) pH dependency of fluorescence lifetime (black squares) and fluorescence intensity (red triangles) for PhOHCl<sub>2</sub>-DAOTA and PhOHCl-DAOTA in RL-100 nanoparticles (10 mM buffer concentration, 140 mM NaCl, 25 °C); b) The pH response for the PSSA nanogel doped with PhOHCl<sub>2</sub>-DAOTA in the same conditions.

### Cell staining/viability

Human colon cancer cells HCT116 were used to investigate staining kinetics, cell viability and pH fluorescence lifetime imaging response of the RL-100 nanoparticles, as described previously.<sup>3,4</sup> The cells were stained with nanoparticles ( $20 \mu\text{g mL}^{-1}$ , 16 h) or free dye ( $150 \text{ ng mL}^{-1}$ , 16 h), washed with growth medium, co-stained with MitoTracker Green (50 nM, 30 min, Molecular Probes) or Calcein Green AM ( $1 \mu\text{M}$ , 30 min) and imaged. Cell viability was tested with a membrane integrity assay with CellTox Green dye (Promega) for nanoparticle concentrations  $0\text{-}50 \mu\text{g mL}^{-1}$  (16 h incubation).

A membrane integrity assay with CellTox Green dye revealed no toxic effects of PhOHCl-DAOTA RL-100 nanoparticles on human colon cancer HCT116 cells, even at concentrations of  $25\text{-}50 \mu\text{g/mL}$  (Figure S-32).

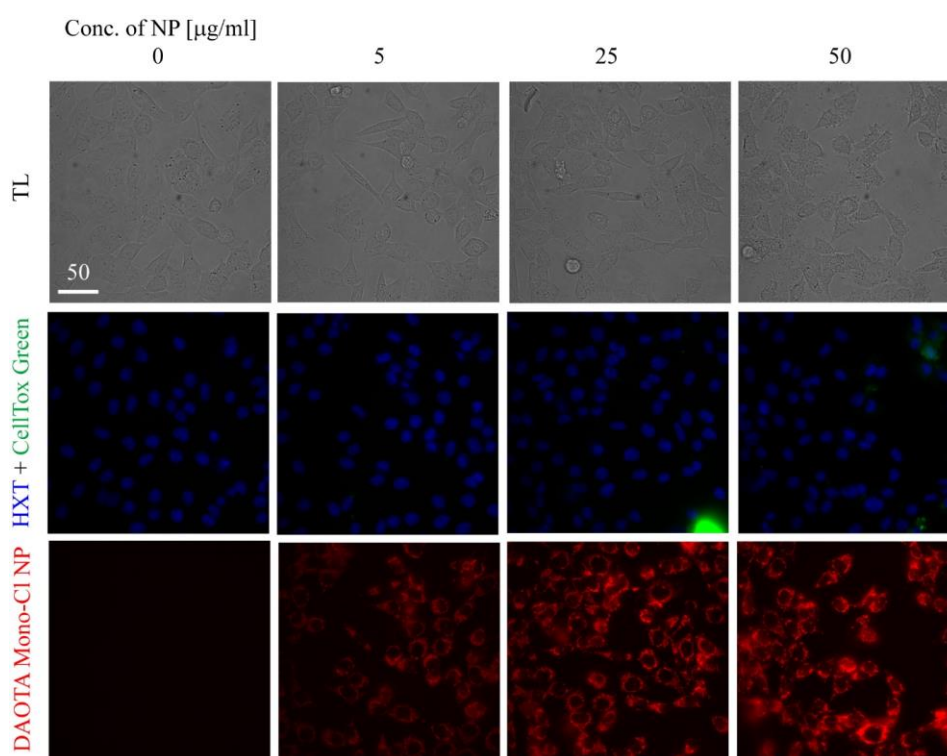


**Figure S 32:** Membrane integrity assay of PhOHCl-DAOTA/RL-100 nanoparticles with CellTox Green dye in human colon cancer HCT116 cells. Cells were incubated with nanoparticles (red,  $0\text{-}50 \mu\text{g/mL}$ , as indicated, 16 h) and counter-stained with Hoechst 33342 (blue, nuclei) and CellTox Green (green, indicates number of dying cells). TL-transmission light. Scale bar in  $\mu\text{m}$ .

RL-100 nanoparticles of PhOHCl-DAOTA displayed quick appearance of fluorescence signals in live cells. Intracellular internalization was evident after one hour (Figure S-33).

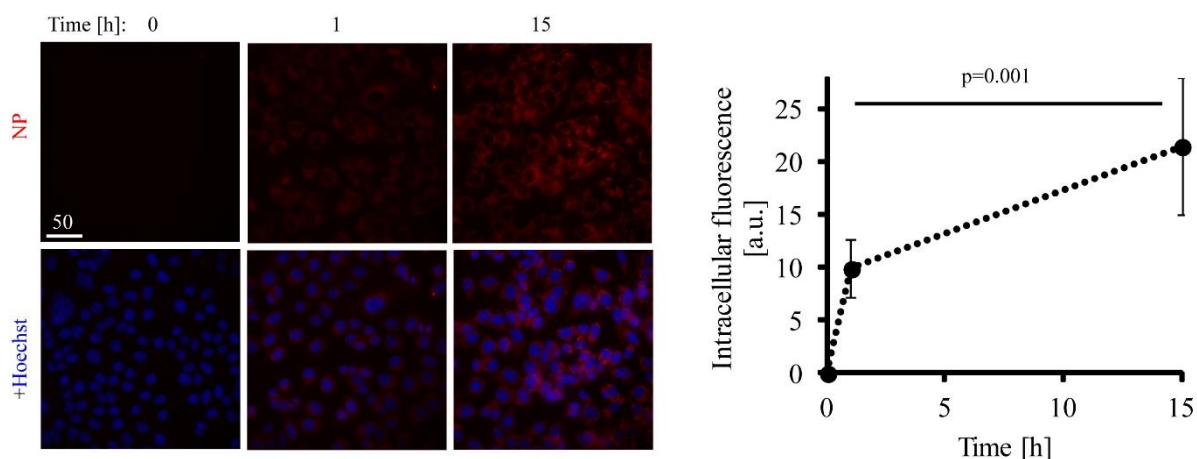


**Figure S 33:** Time-dependence of cell staining of human colon cancer HCT116 cells with PhOHCl-DAOTA nanoparticles in RI-100. Cells were incubated with nanoparticles (10  $\mu\text{g}/\text{ml}$ , red) for indicated time intervals, co-stained with Hoechst 33342 dye (nuclei, blue) washed and immediately imaged. Scale bar in  $\mu\text{m}$ .

Both free dye and RI-100 nanoparticles displayed similarly bright signals and localization inside the cells (Figure S-34).

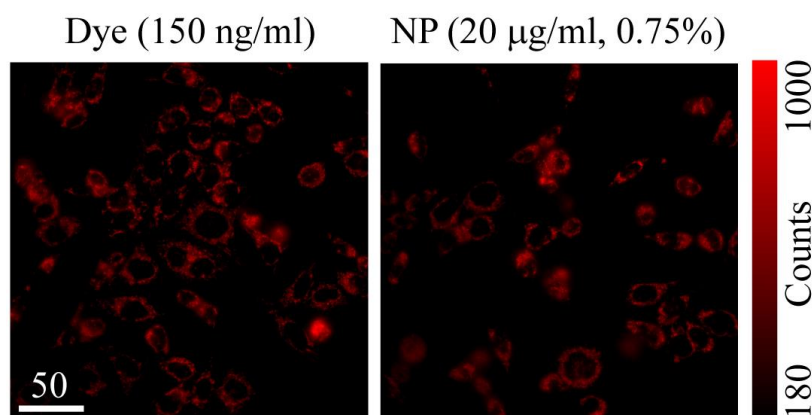


**Figure S 34:** Staining of HCT116 cells with PhOHCl-DAOTA as free dye and RI-100 nanoparticles (NP). Scale bar is in  $\mu\text{m}$ .

When we tested PhOHCl-DAOTA nanoparticle-stained cells in FLIM, we did not observe reliable response to pH changes. Briefly, cells were semi-permeabilized with nigericin (10  $\mu\text{M}$ , 37  $^{\circ}\text{C}$ ) and exposed to KCl-containing pH buffers as described previously<sup>5</sup> (Figure S-35): analysis of distribution histograms shows no expected correlation between pH and fluorescence lifetimes with nanoparticles inside the cells. Interestingly, their localization was similar to mitochondria, however co-staining with MitoTracker Green showed only partial overlap, indicating potential effects of the dye / nanoparticles on the mitochondrial membrane potential or functional status (Figure S-36). In addition, when we treated nanoparticle-stained cells with protonophore FCCP we observed loss of mitochondrial localization for nanoparticles (Figure S-36, bottom).

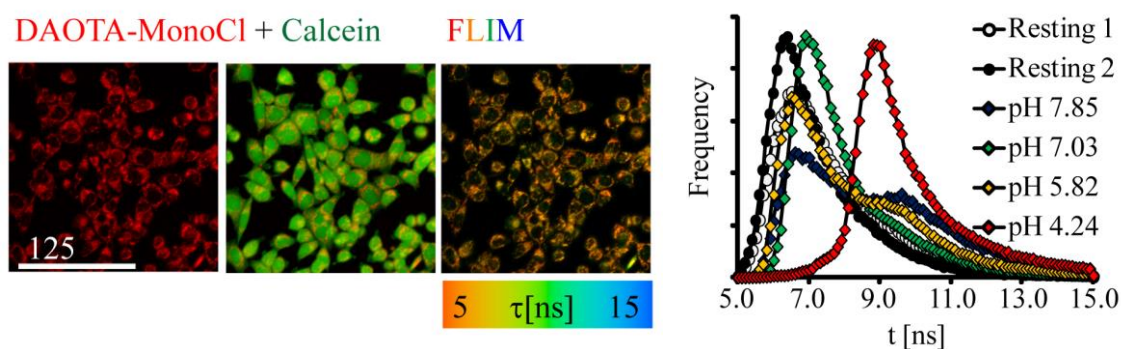


**Figure S 35:** FLIM analysis of pH-dependent response in fluorescence decay time for PhOHCl-DAOTA nanoparticles in live HCT116 cells. Left panel shows characteristic fluorescence intensity of nanoparticles (red), co-stained with Calcein Green AM (1  $\mu$ M, 30 min, green) and false-colour fluorescence lifetime image (scale bar in  $\mu$ m). Right panel shows frequency distribution of fluorescence lifetimes at rest and in cells treated with nigericin and indicated pH buffers.

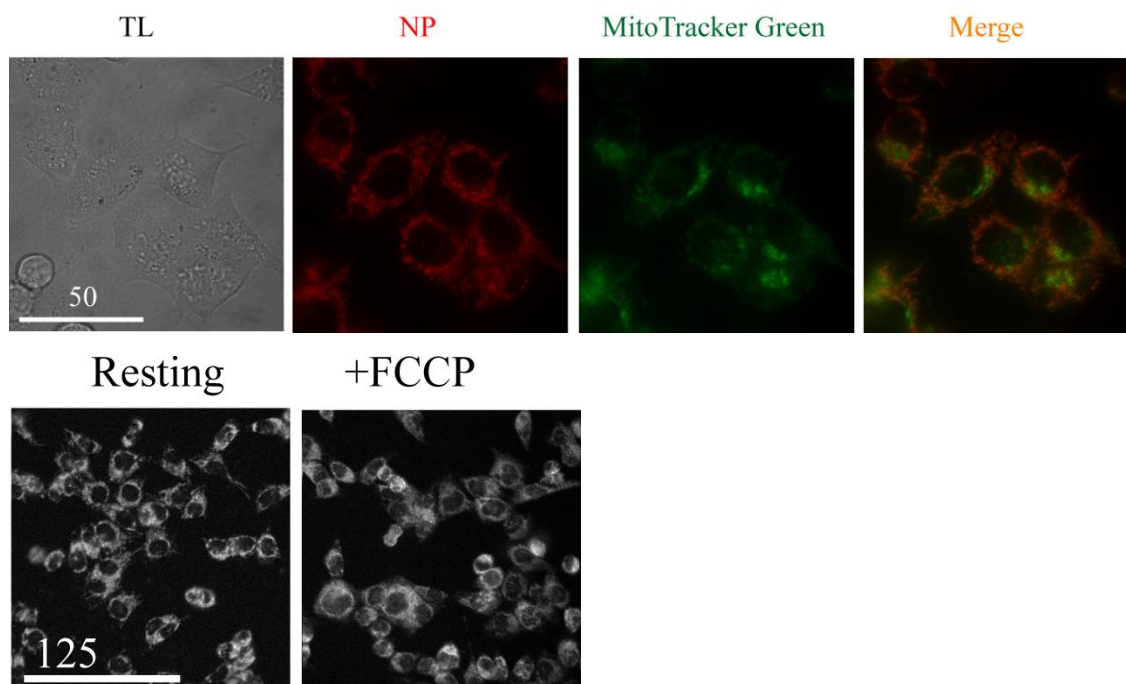


**Figure S 36:** Top: Co-staining of PhOHCl-DAOTA nanoparticles (NP, red) with MitoTracker Green in HCT116 cells. TL- transmission light image. Bottom: Loss of mitochondrial-like localization of PhOHCl-DAOTA RI-100 nanoparticles after application of 2  $\mu$ M FCCP (10 min). (scale bar in  $\mu$ m)

## References

- (1) Fercher, A.; Borisov, S. M.; Zhdanov, A. V.; Klimant, I.; Papkovsky, D. B. Intracellular O<sub>2</sub> Sensing Probe Based on Cell-Penetrating Phosphorescent Nanoparticles. *ACS Nano* **2011**, *5*, 5499–5508.
- (2) Dmitriev, R. I.; Borisov, S. M.; Kondrashina, A. V.; Pakan, J. M. P.; Anilkumar, U.; Prehn, J. H. M.; Zhdanov, A. V.; McDermott, K. W.; Klimant, I.; Papkovsky, D. B. Imaging Oxygen in Neural Cell and Tissue Models by Means of Anionic Cell-Permeable Phosphorescent Nanoparticles. *Cellular and Molecular Life Sciences* **2015**, *72*, 367–381.

- (3) Müller, B. J.; Zhdanov, A. V.; Borisov, S. M.; Foley, T.; Okkelman, I. A.; Tsytsarev, V.; Tang, Q.; Erzurumlu, R. S.; Chen, Y.; Zhang, H.; et al. Nanoparticle-Based Fluoroionophore for Analysis of Potassium Ion Dynamics in 3D Tissue Models and In Vivo. *Advanced Functional Materials* **2018**, *28*, 1704598.
- (4) Dmitriev, R. I.; Borisov, S. M.; Düssmann, H.; Sun, S.; Müller, B. J.; Prehn, J.; Baklaushev, V. P.; Klimant, I.; Papkovsky, D. B. Versatile Conjugated Polymer Nanoparticles for High-Resolution O<sub>2</sub> Imaging in Cells and 3D Tissue Models. *ACS Nano* **2015**, *9*, 5275–5288.
- (5) Aigner, D.; Dmitriev, R. I.; Borisov, S. M.; Papkovsky, D. B.; Klimant, I. PH-Sensitive Perylene Bisimide Probes for Live Cell Fluorescence Lifetime Imaging. *J. Mater. Chem. B* **2014**, *2*, 6792–6801.